Eur. Phys. J. B **7**, 79–83 (1999)

THE EUROPEAN PHYSICAL JOURNAL B

EDP Sciences
© Società Italiana di Fisica
Springer-Verlag 1999

Nonparabolic multivalley balance-equation approach to impact ionization: Application to wurtzite GaN

J.C. Cao[a] and X.L. Lei

China Center of Advanced Science and Technology (World Laboratory) P.O. Box 8730, Beijing 100080, P.R. China
State Key Laboratory of Functional Materials for Informatics, Shanghai Institute of Metallurgy, Chinese Academy of Sciences, 865 Changning Road, Shanghai, 200050, P.R. China

Received: 27 April 1998 / Revised: 17 July 1998 / Accepted: 13 August 1998

Abstract. Extended nonparabolic multivalley balance equations including impact ionization (II) process are presented and are applied to study electron transport and impact ionization in wurtzite-phase GaN with a Γ_1, $L{-}M$, and Γ_2 conduction band structure at high electric field up to 1000 kV/cm. Hot-electron transport properties and impact ionization coefficient are calculated taking account of the scatterings from ionized impurity, polar optical, deformation potential, and intervalley interactions. It is shown that, for wurtzite GaN when the electric field approximately equals 530 kV/cm, the II process begins to contribute to electron transport and results in an increase of the electron velocity and a decrease of the electron temperature, in comparison with the case without the II process. Similar calculations for GaAs are also carried out and quantitative agreement is obtained between the calculated II coefficients by this present approach and the experimental data. Relative to GaAs, GaN has a higher threshold electric field for II and a smaller II coefficient.

PACS. 72.10.-d Theory of electronic transport; scattering mechanisms – 72.20.Ht High-field and nonlinear effects – 72.20.Jv Charge carriers: generation, recombination, lifetime, and trapping

1 Introduction

Recently, extensive experimental investigations on GaN have been made owing to its favorable material properties, such as a large direct band gap, high temperature stability, and high thermal conductivity, which make it an ideal material for blue and ultraviolet electroluminescent devices, and high-temperature/high-power device. Very efficient light-emitting diodes [1], blue lasers [2], short-length InGaN/GaN heterostructure field effect transistors [3], GaN-based superlattices [4] and quantum wells [5], have already been reported. With regard to theoretical studies, as early as 1975, Littlejohn *et al.* [6] performed a calculation of mobility and electron velocity in GaN by using a single-valley Monte-Carlo (MC) model and demonstrated the possible existence of a negative differential mobility at high electric fields. Das and Ferry [7] calculated the average electron velocity of GaN assuming a Maxwellian distribution and showed that the zincblende structure exhibits very different conduction properties from those of the wurtzite structure. Gaskill [8] made an investigation on Hall mobility of wurtzite GaN based on the contraction mapping solution of Boltzmann equation. Recently, either a two-valley [9,10] or a three-valley [11] model is used for simulation of the steady-state electron transport in bulk GaN by an ensemble MC technique and the detailed dependences of drift velocity and intervalley transfer on the electron density, doping concentration, and lattice temperature are shown. However, study of impact ionization (II) process [12] in GaN is relatively lacking.

The balance-equation approach [13] to hot electron transport has recently been extended to include II process and has successfully been used to study II coefficients of bulk InSb [14] with single band structure. The purpose of this work is to extend this II model to multivalley semiconductor systems and apply it to study hot-electron transport and impact ionization in wurtzite GaN at high electric field (up to 1000 kV/cm). The electric field dependence of the electron drift velocity, the average electron energy, and the fractional electron density are calculated and presented with and without the inclusion of the II process. The electron-hole pair generation rate and II coefficient of GaN turn out be in significant difference from those of GaAs obtained by similar calculations.

2 Nonparabolic multivalley balance equations including II process

Considering a semiconductor having a band structure of s valleys with an energy-wavevector relation $\varepsilon_a(\mathbf{k})$ for electrons and $\varepsilon_a^h(\mathbf{k})$ for holes in each valley ($a = 1, 2, ..., s$).

[a] e-mail: jccao@itsvr.sim.ac.cn

$$\mathbf{A}_{ii}^{a}=4\pi\sum_{\mathbf{k},\mathbf{k}',\mathbf{q}}|M_{ii}^{a}(q)|^{2}\,\delta\left(\varepsilon_{a\mathbf{k}-\mathbf{q}}+\varepsilon_{a\mathbf{k}}^{h}+\varepsilon_{a\mathbf{k}'+\mathbf{q}}-\varepsilon_{a\mathbf{k}'}\right)\left[v_{a}\left(\mathbf{k}'+\mathbf{q}\right)+v_{a}\left(\mathbf{k}-\mathbf{q}\right)-v_{a}\left(\mathbf{k}'\right)\right]$$
$$\times f\left(\frac{\overline{\varepsilon}_{a\mathbf{k}'}-\mu_{a}}{T_{a}}\right)\left[1-f\left(\frac{\overline{\varepsilon}_{a\mathbf{k}'+\mathbf{q}}-\mu_{a}}{T_{a}}\right)\right]\left[1-f\left(\frac{\overline{\varepsilon}_{a\mathbf{k}-\mathbf{q}}-\mu_{a}}{T_{a}}\right)\right]\left(1-\frac{f\left[\left(\varepsilon_{a\mathbf{k}}^{h}-\mu_{a}^{h}\right)/T\right]}{f\left[\left(\overline{\varepsilon}_{a\mathbf{k}'}-\overline{\varepsilon}_{a\mathbf{k}'-\mathbf{q}}-\overline{\varepsilon}_{a\mathbf{k}'+\mathbf{q}}+\mu_{a}\right)/T_{a}\right]}\right),\quad(4)$$

$$W_{ii}^{a}=4\pi\sum_{\mathbf{k},\mathbf{k}',\mathbf{q}}|M_{ii}^{a}(q)|^{2}\,\varepsilon_{a\mathbf{k}}^{h}\delta\left(\varepsilon_{a\mathbf{k}-\mathbf{q}}+\varepsilon_{a\mathbf{k}}^{h}+\varepsilon_{a\mathbf{k}'+\mathbf{q}}-\varepsilon_{a\mathbf{k}'}\right)$$
$$\times f\left(\frac{\overline{\varepsilon}_{a\mathbf{k}'}-\mu_{a}}{T_{a}}\right)\left[1-f\left(\frac{\overline{\varepsilon}_{a\mathbf{k}'+\mathbf{q}}-\mu_{a}}{T_{a}}\right)\right]\left[1-f\left(\frac{\overline{\varepsilon}_{a\mathbf{k}-\mathbf{q}}-\mu_{a}}{T_{a}}\right)\right]\left(1-\frac{f\left[\left(\varepsilon_{a\mathbf{k}}^{h}-\mu_{a}^{h}\right)/T\right]}{f\left[\left(\overline{\varepsilon}_{a\mathbf{k}'}-\overline{\varepsilon}_{a\mathbf{k}'-\mathbf{q}}-\overline{\varepsilon}_{a\mathbf{k}'+\mathbf{q}}+\mu_{a}\right)/T_{a}\right]}\right),\quad(5)$$

$$g_{ii}^{a}=4\pi\sum_{\mathbf{k},\mathbf{k}',\mathbf{q}}|M_{ii}^{a}(q)|^{2}\,\delta\left(\varepsilon_{a\mathbf{k}-\mathbf{q}}+\varepsilon_{a\mathbf{k}}^{h}+\varepsilon_{a\mathbf{k}'+\mathbf{q}}-\varepsilon_{a\mathbf{k}'}\right)$$
$$\times f\left(\frac{\overline{\varepsilon}_{a\mathbf{k}'}-\mu_{a}}{T_{a}}\right)\left[1-f\left(\frac{\overline{\varepsilon}_{a\mathbf{k}'+\mathbf{q}}-\mu_{a}}{T_{a}}\right)\right]\left[1-f\left(\frac{\overline{\varepsilon}_{a\mathbf{k}-\mathbf{q}}-\mu_{a}}{T_{a}}\right)\right]\left(1-\frac{f\left[\left(\varepsilon_{a\mathbf{k}}^{h}-\mu_{a}^{h}\right)/T\right]}{f\left[\left(\overline{\varepsilon}_{a\mathbf{k}'}-\overline{\varepsilon}_{a\mathbf{k}'-\mathbf{q}}-\overline{\varepsilon}_{a\mathbf{k}'+\mathbf{q}}+\mu_{a}\right)/T_{a}\right]}\right),\quad(6)$$

Under the influence of a uniform electric field $\mathbf{E}$, the carrier conduction is described by the following equations for the carrier density, effective momentum, and energy balance for each valley ($a=1,2,...,s$, $\hbar=1$ throughout the paper)

$$\frac{dn_a}{dt}-g_{ii}^{a}=\sum_{b(\neq a)}X_{ei}^{ab}+\sum_{b(\neq a)}X_{ep}^{ab},\quad(1)$$

$$\frac{d(n_a v_a)}{dt}=n_a e\mathbf{E}\cdot\mathcal{K}_a+\mathbf{A}_{ei}^{a}+\mathbf{A}_{ep}^{a}+\mathbf{A}_{ii}^{a}+\sum_{b(\neq a)}\mathbf{A}_{ei}^{ab}+\sum_{b(\neq a)}\mathbf{A}_{ep}^{ab},\quad(2)$$

$$\frac{d(n_a\varepsilon_a)}{dt}=n_a e\mathbf{E}\cdot\mathbf{v}_a-W_{ep}^{a}-W_{ii}^{a}-\sum_{b(\neq a)}W_{ep}^{ab}.\quad(3)$$

The above equations are the extension of the balance equations [15,16] to include II process for semiconductors having multiple valleys. The transport state of electrons in the ath valley is described by the electron chemical potential μ_a, the electron temperature T_a and the lattice momentum shift $\mathbf{p}_a$. On the other hand, the drift movement and heating of hole gases are negligible in comparison with those of the electron gases so that the hole gases can be described by the lattice temperature T and a hole chemical potential μ_a^h in each valley ($a=1,2,...,s$). The electron density in ath valley is given by $n_a=1/\left(4\pi^3\right)\int d^3k f\left(\left(\varepsilon_a\left(\mathbf{k}\right)-\mu_a\right)/T_a\right)$. The average velocity $\mathbf{v}_a$, the average energy ε_a, and the ensemble-averaged inverse effective mass tensor $\mathcal{K}_a$ of electron in valley a are defined respectively as $\mathbf{v}_a=\left\langle\nabla\varepsilon_a\left(\mathbf{k}\right)\right\rangle$, $\varepsilon_a=\left\langle\varepsilon_a\left(\mathbf{k}\right)\right\rangle$, and $\mathcal{K}_a=\left\langle\nabla\nabla\varepsilon_a\left(\mathbf{k}\right)\right\rangle$, in which $\langle\cdots\rangle$ stands for the weighted integral over a Brillouin zone in $\mathbf{k}$-space: $\langle\cdots\rangle=1/\left(4\pi^3 n_a\right)\int d^3k f\left(\left(\overline{\varepsilon}_a\left(\mathbf{k}\right)-\mu_a\right)/T_a\right)\cdots$ with $\overline{\varepsilon}_a\left(\mathbf{k}\right)\equiv\varepsilon_a\left(\mathbf{k}-\mathbf{p}_a\right)$ and $f(x)=1/\left[\exp\left(x\right)+1\right]$ the Fermi distribution function. In equations (1, 2, 3), g_{ii}^{a} A_{ii}^{a}, and W_{ii}^{a} are respectively the generation rate, II-induced acceleration, and the II-induced energy-loss rate of ath valley, which describe the contribution of the II process to electron transport. Their expressions are obtained by similar calculation for single valley system [14]

see equations (4, 5, 6) above

in which $\varepsilon_{a\mathbf{k}}^{h}$ is the energy of a hole with momentum $\mathbf{k}$ and μ_a^h is the hole chemical potential in the ath valley. The Fourier representations of the band-band Coulomb interaction matrix element in the ath valley is given by

$$M_{ii}^{a}(q)=\frac{e^2}{\epsilon_0\left(q^2+q_0^2\right)}\frac{I_{cc}I_{cv}}{\kappa},\quad(7)$$

with a dielectric constant κ, and a reciprocal screening length $q_0=\sqrt{n_a e^2/\kappa\epsilon_0 T_a}$. I_{cc} and I_{cv} are overlap integrals of conduction-conduction and conduction-valence bands, respectively. The overall electron average velocity and the average energy are obtained by $v_d=\sum_a n_a v_a/n$ and $\varepsilon=\sum_a n_a\varepsilon_a/n$, respectively, with $n=\sum_a n_a$ the total electron density of the system. The electron-hole generation rate in the whole electron system is expressed by

$$g_{ii}=\frac{\sum_a n_a g_{ii}^{a}}{n},\quad(8)$$

and the II coefficient of the whole electron system is given by

$$\alpha_{ii}=\frac{g_{ii}}{nv}\cdot\quad(9)$$

3 Results and discussions

We have performed a quasi-steady-state calculation of carrier transport in bulk GaN by assuming that the left-hand sides of equations (1, 2, 3) (in which $s=3$) equal zero in the field range of 0–1000 kV/cm. In this quasi-steady-state case, since the momentum- and energy-relaxation

Table 1. Wurtzite-phase GaN parameters used in the calculations.

Band gap (eV)	3.5		
Material density (g/cm^3)	6.1		
Effective hole effective mass (m_0)	1.0		
Longitudinal sound velocity (10^5 cm/s)	4.33		
Static dielectric constant	8.9		
high frequent dielectric constant	5.35		
Acoustic deformation potential (eV)	10.1		
Optical phonon energy (meV)	92.0		
Intervalley phonon energy (meV)	92.0		
Intervalley coupling constant (10^9 eV/cm)	1		
Valley	Γ_1	L–M	Γ_2
Electron effective mass (m_0)	0.19	0.4	0.6
Nonparabolicity (eV^{-1})	0.183	0.065	0.029
Energy separation (eV) (relative to Γ_1 valley)	0	2.0	2.1
Number of equivalent valleys	1	6	1

times are much shorter than the carrier-number relaxation time, the average electron velocity and electron energy become steady while the total number of carriers is still increasing due to II process with a constant rate, namely, the electron-hole pair generation rate g_{ii}^a $(= dn_a/dt)$. We use a three-valley model: Γ_1, L–M, and Γ_2 valleys, for the conduction band of wurtzite-phase GaN, which are obtained from the pseudopotential calculation of band structure [10]. The Kane-type nonparabolic energy-wavevector relation is used for all three conduction bands. The parabolic approximation is assumed for the valence band and the parameters for the hole gas are chosen from the recent experiments [17]. The scattering mechanisms considered here are ionized impurity scattering and phonon scattering from the polar optical, deformation potential, and intervalley interactions. Impact ionization is regarded as an additional scattering mechanism. The role of interband Coulomb scatterings among nonequivalent conduction band is ignored, which is expected to be small when compared to those of electron-phonon scatterings. The material parameters used in the calculation for wurtzite-phase GaN are listed in Table 1, which are from references [10,11,17]. Throughout the paper, the lattice temperature is assumed to be $T = 300\,\mathrm{K}$ and the free electron density of GaN and ionized impurity concentration are set to be $1 \times 10^{17}\,\mathrm{cm}^{-3}$.

For studying II process in semiconductors, Quade *et al.* [18] developed a detailed theory of impact ionization including thresholds for general bands within the hydrodynamic balance-equation approach. They rigorously determined the threshold energy ε_T from momentum and energy conservation for an individual electron. The electron will have a probability to produce an electron-hole pair by II process when its energy is larger than ε_T.

In the present II model, the overlap integral, $I_{cc}I_{cv}/\kappa$, appearing in equation (7) is related to the threshold energy and to electron distribution function, thus it can be,

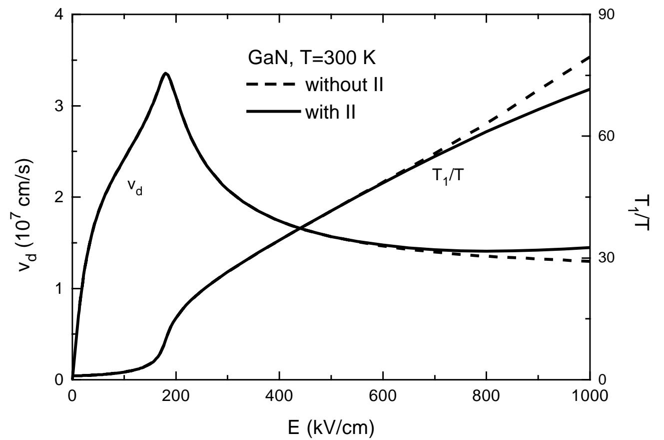

Fig. 1. Calculated average electron velocity, v_d, of the whole system and the normalized electron temperature, T_1/T, for Γ_1 valley as functions of electric field with (solid line) and without (dashed line) II processes. The lattice temperature is $T = 300\,\mathrm{K}$, and the free electron density of GaN and ionized impurity concentration equal $1 \times 10^{17}\,\mathrm{cm}^{-3}$.

in principle, calculated from the energy band structure. In the present study the value of $I_{cc}I_{cv}/\kappa$ is regarded as an adjustable constant. For GaN, we determine the constant by the following ways: (1) without considering the II process, we calculate the electron average energy *vs.* the electric field and find that when the applied electric field $E = 530$ kV/cm the electrons survive to an average energy of 3.51 eV, a value slightly higher than the band gap (3.5 eV) of GaN. We denote this threshold electric field for II as E_T [19,20]. (2) With considering the II process, in order to make the II process contribute to electron transport characteristics (average electron velocity and electron temperature) when $E \simeq E_T$ we find that the value of $I_{cc}I_{cv}/\kappa$ should be 1.12×10^{-3}. Figure 1 shows

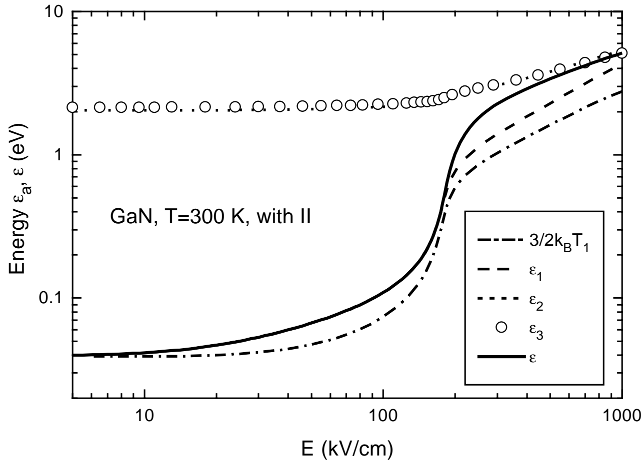

Fig. 2. Average total electron energy, ε, of the system and the average electron energy, ε_a, ($a = 1, 2$, and 3) separate for the Γ_1, $L{-}M$, and Γ_2 valleys are shown as functions of electric field with II process. The classical Boltzmann result $3/2k_BT_1$ is also be plotted for comparison with the average energy, ε_1, of electrons in Γ_1 valley.

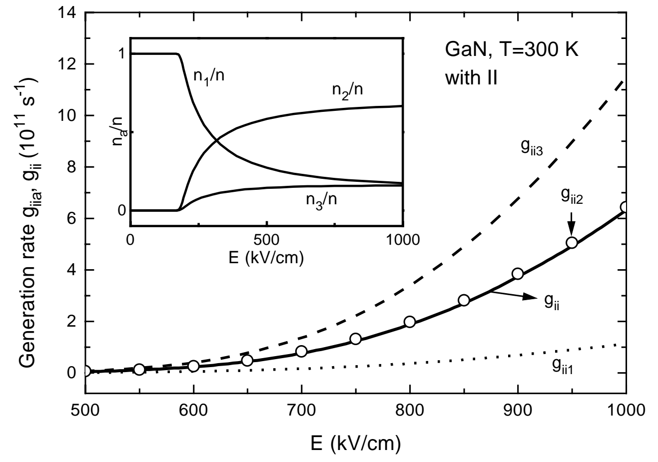

Fig. 3. Calculated average generation rate, g_{ii}, of the whole system and the generation rate, g_{ii}^a, ($a = 1, 2$, and 3) for each valley are shown as functions of electric field. The inset shows the corresponding fractional electron density, n_a/n, for each valley.

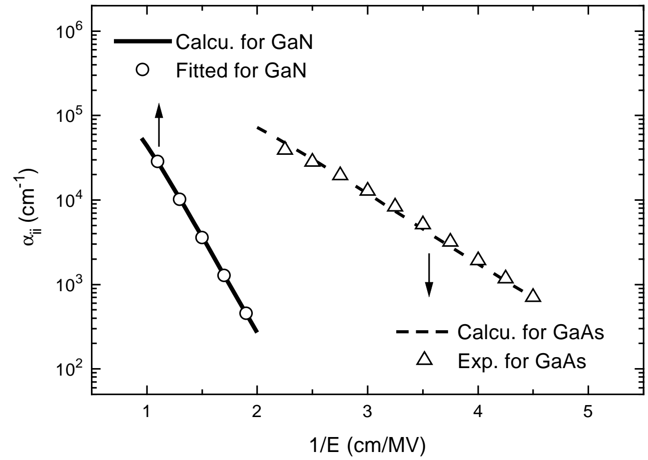

Fig. 4. Calculated II coefficient, α_{ii}, of GaN is shown as a function of the inverse electric field. The open circles is the fitted results by equation (10) for GaN. The II coefficients for GaAs, obtained by similar calculations and by experiments [22], are also plotted for comparison.

the calculated average electron velocity, v_d, of the whole system (left axis) and the normalized electron temperature, T_1/T, for the Γ_1 valley (right axis) as functions of the electric field. The solid line is with the II process while the dashed line is without the II process. Differences between the results with and without II process can be observed for electric fields higher than E_T. The electron temperature is reduced while the electron average velocity is enhanced by II process. The reason is that during the II processes the electron loses at least the gap energy and the remaining total energy of the electron system is redistributed among the newly generated carriers. Both effects reduce electron temperature and consequently increase electron mobility, yielding a higher average electron velocity.

In Figure 2 we show the average total electron energy, ε, of the whole system and the electron energy, ε_a, ($a = 1$, 2, and 3) separate for the Γ_1, $L{-}M$, and Γ_2 valleys as functions of the electric field. In connection with the velocity-field curve, the relation of electron energy vs electric field provides some more physical insight into transport properties, especially into II process. The dependence of the average total energy on electric field in GaN shows a behavior typical for compound semiconductor materials in that the average energy increases abruptly by almost an order of magnitude near the threshold field ($\simeq$ 180 kV/cm) for negative differential mobility with a flattened shape at either the low- or the high-field ranges. It is also shown that at the high-field range the average total electron energy is mainly contributed by the electrons in the $L{-}M$ and Γ_2 valleys. In addition, we also plot in Figure 2 the classical Boltzmann result $3/2k_BT_1$ as function of the electric field. It is found that only at the lower fields less than 10 kV/cm the Boltzmann results are in agreement with the calculated average energy, ε_1, of electrons in the Γ_1 valley, while at the electric fields greater than 10 kV/cm the Boltzmann results are always less than the calculated energy, ε_1. The reason is that the present calculations are based on the Fermi statistics and under the high-field condition the nonparabolicity of energy band plays an important role on electron transport.

The calculated average total generation rate, g_{ii}, of the whole system and the generation rate g_{ii}^a ($a = 1, 2$, and 3) separate for each valleys are shown in Figure 3 as functions of the electric field. Similar to the case in GaAs [21], the II events in GaN mainly originate from the second and third conduction band. At the highest electric field $E = 1000$ kV/cm, g_{ii}^3 is about 10 times as large as g_{ii}^1. The inset shows the corresponding fractional

electron densities in all three valleys with the inclusion of the II process. It can been seen that for a field below the threshold value for the negative differential mobility, more than 97% electrons are distributed in the Γ_1 valley, and for a field above this threshold the population of the Γ_1 valley decreases suddenly, and those of the $L-M$ and Γ_2 valleys increase.

In Figure 4 we show the calculated II coefficient for GaN as a function of the inverse electric field. For comparison, the II coefficients for GaAs, obtained by similar calculations except that the values of $I_{cc}I_{cv}/\kappa$ are determined by fitting the experimental data, are also plotted in this figure. Quantitative agreements of II coefficients for GaAs between the calculated and the experimental data [22] confirm the validity of the present II model. In addition, it is shown that to reach approximately the same II coefficient for GaN, an electric field about 2.4 times as large as that for GaAs, is needed. The dependence of the II coefficient on the electric field E for GaN obeys the empirical formula

$$\alpha_{ii} = \exp\left(-\frac{5175.19\ \text{kV/cm}}{E}\right) 8.46 \times 10^6\ \text{cm}^{-1}, \quad (10)$$

which are plotted in Figure 4 as open circles. Since II coefficient changes by a greater amount with variations in the scattering rate used in the MC calculations, it may difficult to directly compare the present II coefficients with the MC estimates [12]. The experimental work on impact ionization in GaN is highly desirable.

4 Summaries

In conclusion, based on the nonparabolic balance equations extended to II process with multivalley semiconductor structure we have examined electron transport properties and impact ionization effect in wurtzite-phase bulk GaN with a three-valley structure at high electric field up to 1000 kV/cm. Most important transport characteristics, such as electron velocity, electron energy, and intervalley transfer, are calculated taking account of different scattering mechanisms with and without the inclusion of the II process. It is shown that GaN has a higher threshold electric field for impact ionization and a smaller II coefficient when compared to GaAs, which makes it one of the best materials for high-power device applications.

The work is supported by the National Natural Science Foundation of China, National and Shanghai Municipal Commissions of Science and Technology, and the Shanghai Foundation for Research and Development of Applied Materials.

References

1. S. Nakamura, T. Mukai, M. Senoh, Appl. Phys. Lett. **64**, 1687 (1994).
2. S. Nakamura, M. Senoh, S. Nagahama, N. Iwasa, T. Tamada, T. Matsushita, H. Kiyoku, Y. Sugimoto, Jpn J. Appl. Phys. **35**, L74 (1996).
3. M.A. Khan, Q. Chen, M.S. Shur, B.T. Dermott, J.A. Higgins, J. Burm, W. Schaff, L.F. Eastman, IEEE Electron Dev. Lett. **17**, 584 (1996).
4. M.A. Khan, J.N. Kuznia, D.T. Olson, T. George, W.T. Pike, Appl. Phys. Lett. **63**, 3470 (1993).
5. M.A. Khan, R.A. Skogman, J.M. Van Hove, S. Krishnankutty, R.M. Kolbas, Appl. Phys. Lett. **56**, 1257 (1990).
6. M.A. Littlejohn, J.R. Hauser, T.H. Glisson, Appl. Phys. Lett. **26**, 625 (1975).
7. P. Das, D.K. Ferry, Solid-State Electron. **19**, 851 (1976).
8. D.K. Gaskill, K. Doverspike, L.B. Rowland, D.L. Rode, Inst. Phys. Conf. Ser. **141**, 425 (1994).
9. N.S. Mansour, K.W. Kim, M.A. Littlejohn, J. Appl. Phys. **77**, 2834 (1995).
10. J. Kolnik, I.H. Oguzman, K.F. Brennan, R. Wang, P.P. Rudan, Y. Wang, J. Appl. Phys. **15**, 1033 (1995).
11. U.V. Bhapkar, M.S. Shur, J. Appl. Phys. **82**, 1649 (1997).
12. J. Kolnik, I.H. Oguzman, K.F. Brennan, R. Wang, P.P. Ruden, J. Appl. Phys. **81**, 726 (1997).
13. X.L. Lei, C.S. Ting, Phys. Rev. B, **32**, 1112 (1985); X.L. Lei, N.J.M. Horing, H.L. Cui, Phys. Rev. Lett. **66**, 3277 (1991); X.L. Lei, Phys. Stat. Sol. b **170**, 519 (1992).
14. X.F. Wang, X.L. Lei, J. Phys.-Cond. **7**, 7871 (1995).
15. X.L. Lei, D.Y. Xing, M. Liu, C.S. Ting, J.L. Birman, Phys. Rev. B **36**, 9134 (1987).
16. X.L. Lei, J.C. Cao, B. Dong, J. Appl. Phys. **80**, 1504 (1996).
17. M. Steube, K. Reimann, D. Fröhlich, S.J. Clarke, Appl. Phys. Lett. **71** 948 (1997).
18. W. Quade, E. Schöll, M. Rudan, Solid-State Electron. **36**, 1493 (1993).
19. W. Shockley, Solid-State Electron. **2**, 35 (1961).
20. Y.C. Chen, P.K. Bhattacharya, J. Appl. Phys. **73**, 465 (1993).
21. M.V. Fischetti, S.E. Laux, Phys. Rev. B **38**, 9721 (1988).
22. G.E. Bulman, V.M. Robbins, G.E. Stillman, IEEE Trans. Electron Dev. **ED-32**, 2454 (1985).